GAS DYNAMICS OF IMPULSIVE JETS AND PRESSURE OSCILLATIONS OF A LASER-IRRADIATED TARGET

N. M. Bulgakova
and L. I. Kuznetsov

UDC 533.6.011:535.211

1. Introduction. The interaction of an intense millisecond pulse of laser radiation (LR) with a solid target can be accompanied by pressure oscillations, recorded by a piezoelectric transducer on the backside of the irradiated target, with frequencies of the order of 10 kHz [1]. This phenomenon occurs on a lead target with LR intensity of about 2 MW/cm^2. In [2] it is shown that pressure oscillations are observed on different dielectric and metallic targets in a wide range of LR energies and is accompanied by intense vaporization of the material in the irradiation spot. Possible mechanisms for the appearance of these oscillations are suggested in [3, 4]: bursts of absorption in the plasma in an unstable vaporization regime or auto-oscillatory regime of self-screening of the LR by the products of erosion. Probe measurements through a narrow channel in the target under high pressures of the surrounding medium have shown that oscillations of absorption of the LR in the photoerosion flame are observed in the tail part of the oscillograms in some irradiation regimes [5]. These absorption oscillations can be interpreted in a manner supporting the above-mentioned mechanism of the pressure oscillations on iradiated targets [3].

However, investigations of the attenuation of radiation in the photoerosion flame of ebonite and magnesium targets in air with LR intensities such that pressure oscillations should be observed indicate that there are no pronounced pulsations of the absorption coefficient for laser radiation through the photoerosion flame [6]. Finally, simultaneous measurements of the pressure on the target and LR attenuation by the photoerosion flame [7] have shown that the LR transmission curves are quite smooth, and the small nonmonotonic variations on these curves are not related with the pressure oscillations on the target. These investigations, as well as measurements performed with different irradiation configurations [8] and change in sign of the pressure vector [2] have made it possible to propose a gas-dynamic mechanism for the appearance of the pressure oscillations on irradiated targets.

In the present work, in order to check this mechanism we performed numerical modeling of the gas dynamics of an erosion flame and compared the computational and experimental results in a wide range of irradiation intensities.

2. Experimental Procedure. Detailed experimental investigations of the pressure on irradiated targets were performed on a VIKA vacuum chamber [9]. The 1.06 μm laser pulses with a width of 0.3 msec at half-height was focused on the target through a long focal length lens. The diameter of the irradiation spot ranged from 5 to 20 mm, and the target had a diameter of 20 mm. The target was placed on a piezoelectric transducer [10], which measured the pressure on the irradiated target.

A coaxial FK-19 photocell was used to record the initial laser radiation from a beam splitter placed at the output of the laser system. The signals from the piezoelectric transducer and from the FK-19 photocell were fed into an S9-8 two-channel digital oscillograph. The data were transmitted from the oscillograph to an IVK-6 measurement–computing system through a KOP interface. Processing of the signals from the piezoelectric transducer on the IVK-6 system consisted of dividing the area under the oscillogram into 10-μsec long elementary sections and normalizing these elementary areas P_i twice – with respect to both the total area ΣP_i under the oscillogram and the energy E_0, normalized in the same manner, of the initial laser radiation: $\tilde{P} = (P_i/\Sigma P_i)/(E_{0i}/\Sigma E_{0i})$. Processing in this manner makes it possible to reveal, irrespective of the shape of the laser pulse and the magnitude of the signals, the characteristic behavior of the pressure forces acting on the target at frequencies below 100 kHz and it corresponds to the total overall pressure on the target, normalized to the pressure in the irradiation spot.

Novosibirsk. Translated from Prikladnaya Mekhanika i Tekhnicheskaya Fizika, No. 6, pp. 14-21, November-December, 1992. Original article submitted July 5, 1991.

 0021-8944/92/3306-0780$12.50

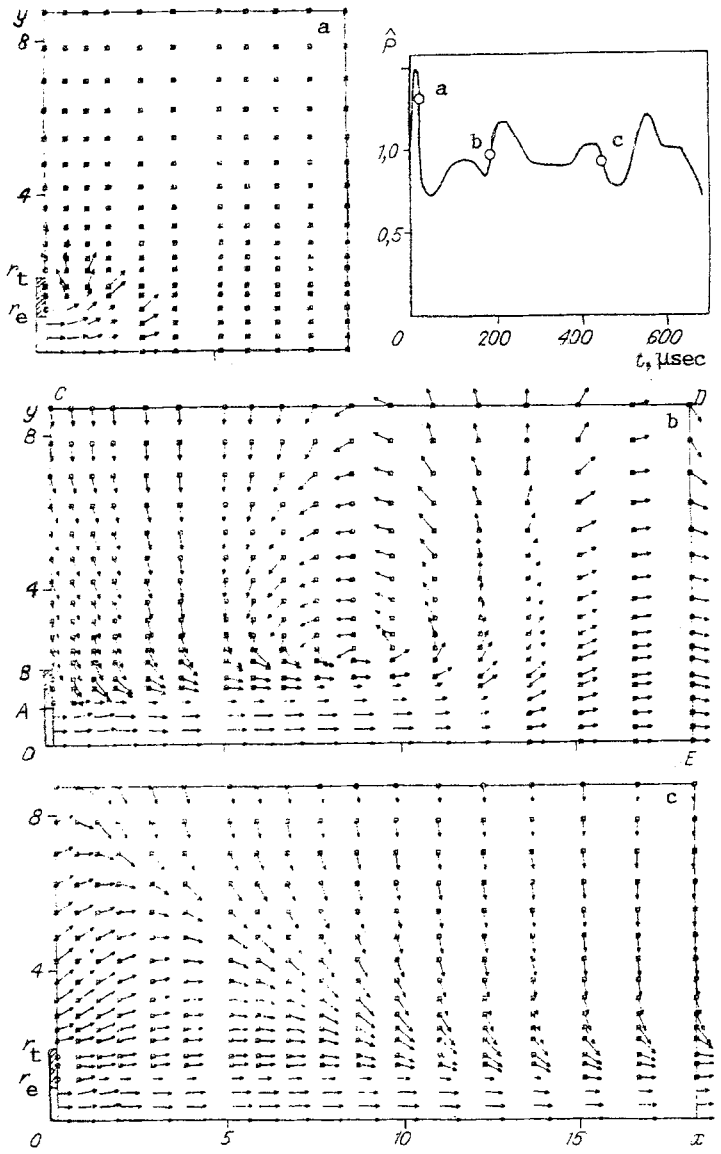

Fig. 1

3. Numerical Modeling. A numerical calculation of the gas-dynamic picture of an impulsive process such as a quasistationary erosion flame in a submerged space can be performed only on the basis of the complete system of Navier–Stokes equations, since gas from the submerged space is entrained in the motion and regions of subsonic flow, which can significantly influence the structure of the entire flow, are formed.

The following model was adopted for the erosion flame. For simplicity, the appearance of the flame was modeled by instantaneous actuation of a sonic nozzle. The time during which the target surface is heated up to the start of intense vaporization and the shape of the laser pulse were neglected. It was assumed that the products of erosion are not ionized. Ionization and recombination processes affect the position of the shocks [11], but the flow is qualitatively similar in cases with and without plasma. Since a quite dense gas and moderate laser radiation intensities are considered, so that the degree of ionization of the products of erosion is low, collective effects in the plasma will not be noticeable.

In the present work we did not consider the problem of obtaining complete quantitative agreement between the calculations and the experiment. The object of this work was to determine the possibility for the appearance of pressure oscillations on a target on the basis of only the gas dynamics of an erosion flame neglecting boiling processes on the surface, absorption of radiation by the products of erosion, and plasma effects.

The complete system of Navier–Stokes equations for the case of cylindrical symmetry was used. The system was solved numerically by the method of setting, using an implicit splitting

scheme [12, 13]. The scheme was written in a form similar to [14] and approximates the initial system of equations with first-order equations in the nonstationary case [13].

The problem was solved in the upper half-plane from the symmetry axis OE (Fig. 1b), on which the conditions of flow symmetry were imposed:

$$\frac{\partial \rho}{\partial y} = \frac{\partial u}{\partial y} = v = \frac{\partial e}{\partial y} = 0.$$

Here x and y are coordinates in a rectangular coordinate system (x is measured along the axis of the flame); ρ is the density; e is the internal energy; and, u and v are the longitudinal and transverse components of the velocity.

The region of integration was bounded on the left by the irradiation spot OA (by the sonic nozzle), adjoining the spot of the solid surface (unirradiated edge of the target) AB, on which attachment conditions were imposed:

$$u(0, y) = v(0, y) = 0, \quad T(0, y) = T_w = \text{const}, \frac{\partial p_s}{\partial x}\Big|_{x=0} = 0$$

where $p_s = nT$ is the static pressure. The condition of "free efflux" was imposed above the target on the boundary BC:

$$\frac{\partial f}{\partial x} = 0 \quad \text{or} \quad \frac{\partial^2 f}{\partial x^2} = 0, \quad f = (\rho, u, v, e).$$

The size of the target was varied in the calculations. The top boundary CD was positioned far enough away from the axis so that the gas in the submerged space could be treated as undisturbed. In the case of jet effluxes in a vacuum the conditions of "free efflux" (with derivatives along the y axis) were also imposed on the top boundary. The same conditions were imposed on the right-hand boundary DE, which was positioned at a distance greater than $20r_e$, where r_e is the radius of the irradiation spot, from the target. Initially, the entire region of integration was assumed to be undisturbed and the conditions $f_e = (\rho_e, u_e, 0, e_e)$ were imposed at the edge of the sonic nozzle. The system of equations was normalized to the parameters in the irradiation spot r_e, ρ_e, and u_e. The problem was solved on a strongly nonuniform grid. The grid steps along the x and y axes increased with increasing distance from the irradiation spot. The conditions of such a calculation are described in greater detail in [15].

4. Flow Field and Pressure Pulsations on the Target. Before the erosion flame is activated the force (total pressure) acting on the target is zero. It was assumed that the target is infinitely thin (the side surfaces of the target were neglected) and the gas on the opposite side of the target is stationary. Figure 1 displays the computational results for the case when the target size $r_t = 2r_e$, the ratio of the temperatures at the nozzle edge and in the surrounding space $T_e/T_\infty = 2$, the degree of off-design $n = 2$ ($n = p_e/p_\infty$, where p_e is the pressure at the nozzle edge), and Reynolds number $Re = 10^3$. The total pressure on the target, normalized to the reaction force P_j of the jet,

$$\hat{P} = \int_S p dS / P_j.$$

is plotted as a function of time. Here p is the local pressure on the target: $p = p_s + p_d$; $p_s = nT$ is the static pressure; $p_d = -nmu|u|/2$ is the dynamic correction to the pressure on the target; the velocity component u was chosen at a point of the grid next to the target; and, $\hat{P} = \hat{P}_s + \hat{P}_d$. The points a-c are the times at which the corresponding flow fields are indicated in Figs. 1a-c.

At the moment the jet is activated, the total pressure on the target is equal to the reaction force of the jet. Next, due to the expansion of the erosion products into the submerged space at lower pressure and entrainment of the gas surrounding the target into motion, the pressure on the target has a peak, which transforms into pulsations. A similar picture is observed when a rocket engine is fired [16] and the bottom of the rocket is subjected to strong pressure oscillations.

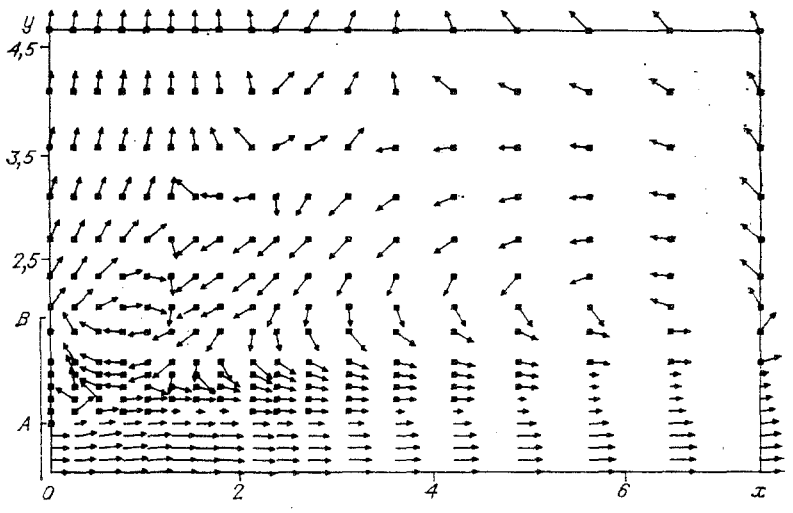

Fig. 2

Before analyzing the flow fields, we note that the graphics system SIGAM [17] employed automatically normalizes the velocity vector to the maximum velocity in a given array of velocities. The system chooses the length of an arrow so that the arrow falls within the grid square assigned to it. For the grid employed in the present work, if in drawing the vector flow fields the modulus of the velocity vector is less than 15% of the maximum value, the vector is drawn with the established length and a square is drawn at its base. Vectors close to the maximum vector are drawn without a square at the base.

The flow field in Fig. 1a corresponds to 25 μsec after the moment the erosion flame is activated. As the jet expands, it entrains the surrounding gas. Backflow arises behind the target. In addition, the target is subjected to dynamical pressure, since near the target the velocity vector has a component along the flow axis, directed toward the target. The flow fields in Figs. 1b and c correspond to 190 and 430 μsec. The calculations showed that when the jet is activated impulsively a vortex forms in the submerged space near the exit opening (irradiation spot) and then moves along the jet. A well-formed vortex flow, which in our case is cylindrically symmetric and has the shape of a torus, can be seen clearly in Fig. 1b. By 430 μsec the vortex leaves the region of computation in the direction of the jet.

The behavior of the pressure near the target is undoubtedly associated with the vortex flow, since the vortex affects the direction of the velocities. Thus, the field of the flow in Fig. 1b corresponds to a pressure increase near the surface and the flow field in Fig. 1c corresponds to a pressure decrease. It is obvious that in the first case the vortex causes gas to flow from the periphery to the surface of the target, whence gas is pulled by the jet due to viscosity, while in the second case the gas flows away from the surface and a low-pressure region appears at the target.

The number of pulsations is not associated with the number of vortices formed. In the case shown in Fig. 1, only one vortex appears and the pulsational behavior of the jet is due to the setting process (re-expansions and subsequent compressions). The calculations showed that the vortex structure arises when the pressure undergoes sharp oscillations (in Fig. 1 a vortex is formed at the end of the first peak of the pulsations). Under some conditions such sharp pressure pulsations can arise repeatedly during the process of establishing a jet, and then a multivortex structure forms. The vortices formed at the target surface follow one another along the jet. Figure 2 displays an enlarged fragment of such a flow near the target with the initial data as in Fig. 1 but with $T_e/T_\infty = 4$.

5. Mechanism of the Pulsations. As we have already mentioned above, the total normalized pressure on target $\hat{P}$ consists of the static pressure $\hat{P}_s$ and the dynamic pressure $\hat{P}_d$, acting on the unirradiated edge of the target, and the thrust of the jet $\hat{P}_j$ ($\hat{P}_j = 1$ in the calculations). Figures 3a-c display plots of $\hat{P}$ and its components, respectively, for n = 2, 25, and 50; Fig. 3d is a time-stretched fragment of the start of the curves in Fig. 3c. The dots represent the experimental curves of the total normalized pressure. Obviously, it is mainly the static pressure that pulsates, while the dynamical pressure remains quite even, undergoing weak oscillations in antiphase to the static pressure. Since according to the calculations

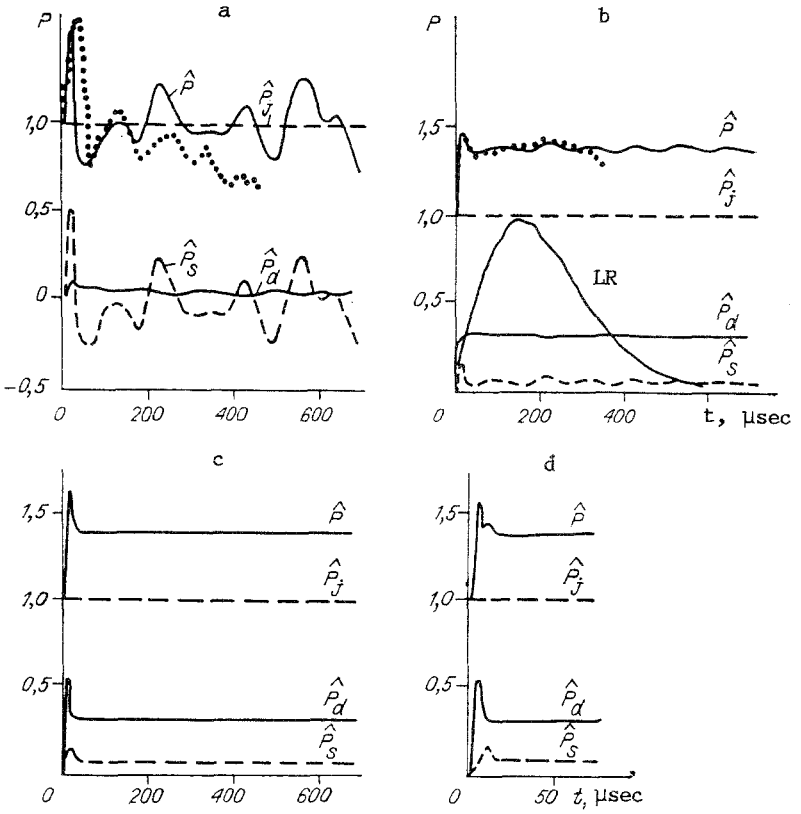

Fig. 3

the behavior of the temperature near the target is monotonic, the pressure pulsations are produced by the gas flowing into and out of the surface region (density oscillations). As the degree of off-design increases, these pulsations decay. As mentioned above, the pressure pulsations are associated with the process of setting the jet. The calculations showed that the jet setting time τ_s decreases from 1500 to 350 μsec as the degree of off-design increases from 2 to 50. For n = 50 the pressure near the target stabilizes even more rapidly – immediately after the first peak. Thus for n = 2 there is not enough time for the jet to reach a stationary state during the laser pulse (600 μsec). Conversely, at n = 50 the jet stabilizes rapidly. In the experiment, however, pressure pulsations are still possible with such degrees of off-design [2], since in the calculation the flow rate is constant while in the experiment the flow rate first increases and then starts to decrease as the laser pulse decays (laser radiation curve in Fig. 3b); this is what drives the jet out of the stationary state. On the whole, however, as the degree of off-design increases, the amplitude of the pulsational component of the total pressure decreases.

One can see in Fig. 3a that the first peaks of the static and dynamical pressure coincide, after which they start to oscillate in antiphase. As the degree of off-design increases, the first peak of the static pressure lags behind the dynamical pressure, due to which the first peak of the total pressure splits off (Fig. 3d), which seemingly doubles the frequency of the first pulsation. This is evidently the explanation obtained for the splitting of the first pulsation peaks in experiments with laser irradiation of dielectrics and metals [2, 18, 19]. On the whole, the experimental curves agree qualitatively with the computed curves. This shows that the gas-dynamic mechanism of the pulsations is well-founded.

Another confirmation of this mechanism is the fact that the pulsations contain a negative total pressure on target, something that cannot be explained on the basis of the propositions made in [3, 4]. Figure 4 displays an example of such a regime, in which there arise pulsations with a negative force acting on the target. The plot corresponds to the parameters $r_t = 2r_e$, $T_e/T_\infty = 2$, n = 1.1, and $Re = 10^3$. The dots are the experimental points and the solid curve represents the computed total normalized pressure on the target. It is interesting that the oscillation amplitude has increased even more with decreasing n.

6. Conservatism of the Pulsational Component with Respect to the External Pressure. We underscore the fact that it is the use of normalization to the reaction force of the jet P_j that gives an increase in the oscillation amplitude with decreasing degree of off-design,

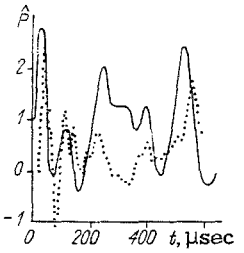

Fig. 4

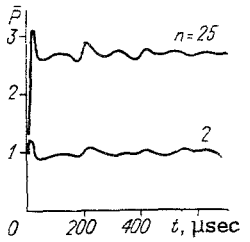

Fig. 5

which can change both due to the pressure in the irradiation spot (LR intensity) and the pressure in the submerged space. For P_j = const and therefore with constant LR intensity and variable p_∞ this corresponds to the real behavior of the absolute amplitude of the pulsations. When, however, p_∞ = const and P_j is variable, the normalization to P_j distorts the real picture and normalization is best performed with respect to the constant quantity p_∞, especially since, as shown above, it is the gas pressure of the submerged space near the unirradiated edge of the target that determines the oscillations of the total pressure. Since in the calculations, after the jet is activated, P_j is constant and independent of the time t, for convenience of analysis we subtract the component P_j from the total pressure, and we normalize the remaining forces acting on the target to p_∞:

$$\bar{P} = 2\pi \int_{r_e}^{r_t} prdr/p_\infty.$$

Figure 5 shows the results of such analysis for $r_t = 2r_e$, $T_e/T_\infty = 2$, and $Re = 10^3$. The total pressure on the unirradiated edge of the target obviously increases with increasing n; this is mainly associated with the dynamical component of the pressure accompanying expansion of the erosion products into a lower-pressure region. There is some increase in the oscillation amplitude $\bar{P}$ with increasing degree of off-design. This can be explained by the increase in the intensity of the jet, which in turns entrains more strongly the surrounding gas. However, the fact that the amplitude of the oscillations $\bar{P}$ does not increase much with n increasing by more than an order of magnitude with fixed p_∞, also supports the fact that the pulsations are determined mainly by the motion of the gas surrounding the target and not by the erosion flame. This result agrees with the experimental investigations of the conservative nature of the oscillation amplitudes relative to p_∞ in a wide range of values of n [2].

Thus, it has been shown that the main mechanism of pulsations of the pressure on a target irradiated with a powerful laser pulse is entrainment of the gas in the submerged space and the effect of the gas on the unirradiated edge of the target.

The flame model employed for calculating the complete system of Navier–Stokes equations was extremely simplified: the shape of the laser pulse, possible oscillations in the intensity of the laser radiation, ionization processes, absorption of the radiation by products of erosion, nonuniform distribution of the energy in the irradiation spot, and many other factors were neglected. Taking these factors into account could change the picture of the pulsations. However, the numerical calculation performed and the flow fields give a graphic representation of the gas-dynamic processes occurring in the space around the flame, and the good agreement between the calculations and the experimental data shows that such a simple model reflects correctly the main mechanism responsible for the appearance of pressure pulsations on the target. In addition, it explains the possibility of the appearance of negative pressure peaks, the pronounced first peak of the pulsations, the decrease in the relative amplitude of pulsations with increasing irradiation energy, and the conservative nature of these pulsations with respect to the pressure of the surrounding medium.

LITERATURE CITED

1. B. M. Zhiryakov, N. I. Popov, and A. A. Samokhin, "Effect of plasma on the interaction of laser radiation with a metal," Zh. Éksp. Teor. Fiz., 75, No. 2(8) (1978).
2. L. I. Kuznetsov, "Pressure oscillations on a target irradiated with a laser pulse," Zh. Tekh. Fiz. 60, No. 8 (1990).
3. A. A. Uglov and S. V. Selishchev, Auto-oscillatory Processes Accompanying Action of Concentrated Energy Fluxes [in Russian], Nauka, Moscow (1987).

4. A. A. Samokhin, "First-order phase transitions accompanying interaction of laser radiation with an absorbing condensed medium," Tr. IOFAN [in Russian], Nauka, Moscow (1988), Vol. 13.
5. A. A. Uglov and M. B. Ignat'ev, "Optical characteristics of a laser plasma near the surface of a solid target in high-pressure gases," Fiz. Plazmy, 8, No. 6 (1982).
6. L. I. Kuznetsov, "Screening of a laser pulse in a photoerosion flame of metallic and dielectric targets," Zh. Prikl. Spektrosk., 53, No. 6 (1990).
7. L. I. Kuznetsov, "Interaction of photoerosion flame with the surrounding medium and pressure oscillations on an irradiated target" in: Abstracts of Reports at the 8th All-Union Conference on the Interaction of Optical Radiation with Matter, GOI, Leningrad (1990), Vol. 2.
8. L. I. Kuznetsov, "Transfer of a pressure pulse to metallic and dielectric target irradiated with a neodymium laser in the free-lasing mode," Prikl. Mekh. Tekh. Fiz., No. 6 (1991).
9. S. S. Kutateladze, L. I. Kuznetsov, and V. I. Zav'yalov, "VIKA pulsed vacuum chamber" in: Abstracts of Reports at the 4th All-Union Conference on the Dynamics of Rarefied Gases, Inst. Termofiz. Sib. Otdel. Akad. Nauk SSSR, Novosibirsk (1979).
10. E. S. Voronel', L. P. Kiryuship, and L. I. Kuznetsov, "Measurement of pulsed pressure on targets accompanying formation of photoerosion flame," Sib. Fiz.-Tekh. Zh. (Izv. SO RAN), No. 2 (1991).
11. N. M. Bulgakov, "Expansion of a plasmoid into the atmosphere" in: Nonequilibrium Processes in Single- and Two-Phase Systems [in Russian], Inst. Termofiz. Sib. Otdel. Akad. Nauk SSSR, Novosibirsk (1981).
12. Yu. A. Berezin, V. M. Kovenya, and N. N. Yanenko, "An implicit scheme for flow of a viscous heat-conducting gas," ChMMSS, 3, No. 4 (1972).
13. Yu. Berezin, V. M. Kovenya, and N. N. Yanenko, "Difference method for solving problems of flow past bodies in "natural" coordinates" in: Aéromekhanika [in Russian], Nauka, Moscow (1976).
14. B. D. Kovalev and V. I. Myshenkov, "Calculation of a viscous supersonic jet effluxing into a heated space," Uchen. Zap. TsAGI, 9, No. 3 (1978).
15. N. M. Bulgakov, "Numerical modeling of pulsed jets of viscous heat conducting gas," Prikl. Mekh. Tekh. Fiz., No. 4 (1992).
16. M. C. Cline and R. G. Wilmoth, "Computation of the space shuttle solid rocket booster nozzle start up transient flow," AIAA Paper No. 84-0462, New York (1984).
17. Methodological Recommendations for Use of the SIGAM Graphics System [in Russian], SNIIGGiMS Novosibirsk (1988).
18. L. I. Kuznetsov, "Interaction of a photoerosion flame with the surrounding medium," Izv. Akad. Nauk SSSR, Ser. Fiz., No. 6 (1991).
19. L. I. Kuznetsov, "Passage of radiation through a laser plasma and pressure pulsations on targets," Sib. Fiz.-Tekh. Zh. (Izv. SO RAN), No. 1 (1992).